ECAS 2016

sciforum

Conference Proceedings Paper

Interannual Variation of a 12,760 km Transequatorial Ionospheric Channel Availability and Its Dependence on Ionization

Ferran Orga [1,*], David Altadill [2], Marcos Hervás [1] and Rosa Ma Alsina-Pagès [1]

Published: 15 July 2016

[1] GTM—Grup de Recerca en Tecnologies Mèdia, La Salle – Universitat Ramon Llull, Barcelona, Spain; mhervas@salleurl.edu (M.H.); ralsina@salleurl.edu (R.M.A.-P.)
[2] Observatori de l'Ebre, CSIC – Universitat Ramon Llull, Barcelona, Spain; david_altadill@obsebre.es
* Correspondence: forga@salleurl.edu; Tel.: +34-932-902-455

Abstract: The ionosphere provides a channel able for long-haul and Non-Line-Of-Sight (NLOS) communications. Nonetheless, the amount of ionization depends on the Sun activity, whose diurnal and seasonal cycles transform the channel constantly. La Salle and the Observatori de l'Ebre have been sounding a 12,760 km ionospheric channel from Antarctica (62.7°S, 299.6°E) to Spain (41.0°N, 1.0°E) in order to find this evidence and to analyze the characteristics of this particular channel. The final goal of the project is to establish a stable communications link to be used as backup or for low rate data transmission. The aim of this paper is to prove the relation between the channel availability and the Sun phenomena affecting the ionization in four consecutive sounding campaigns.

Keywords: ionospheric propagation; HF; long-haul; sounding; sun activity; ionization; SSN; SNR; channel availability

1. Introduction

The ionosphere is a very hostile channel for radio communication due to the several phenomena changing its propagation conditions continuously. The amount of ionization varies considerably depending on the Sun's activity, thus, variations of the flux of the solar ionizing radiations as Ultraviolet and X-rays, as well as variations in the solar particle emissions can cause significant ionospheric effects [1] that, in turn, have a great interest when modeling the ionospheric channel [2]. These solar activity variations are mainly caused by the 11-year solar cycle and solar rotation but diurnal and seasonal variations play a significant role in the ionospheric variability also [3]. In [4] the possible causes of the ionospheric variability are summarized, ranging from time-scales of minutes (e.g., Traveling Ionospheric Disturbances, TID's) to long-term changes (solar cycle variations and even secular). [5,6] have evaluated the ionospheric variations shorter that 18 days period and its impact and contribution to the ionospheric variability.

La Salle and the Observatori de l'Ebre have been sounding the 12,760 km ionospheric channel (see Figure 1) from Antarctica (62.7°S, 299.6°E) to Spain (41.0ººN, 1.0°E) during the last 11 years [7]. During the austral summer, the oblique ionosonde was deployed annually by our team in the Livingston Island (South Shetland Archipelago). The transmitter antenna built there is a 7.5 m rugged monopole fed only with 250 W due to environmental restrictions. In Cambrils (Spain), the results of the soundings were received using the above-mentioned monopole and an inverted-V antenna.

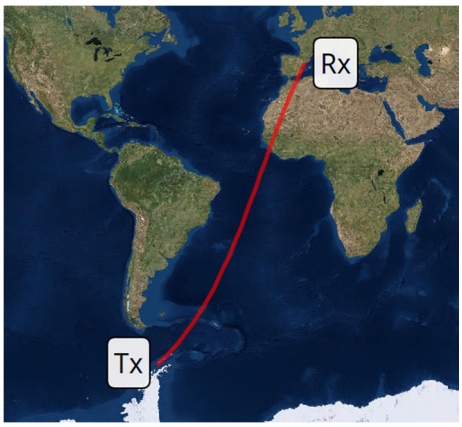

Figure 1. The 12,760 km link over the map with the Receiver (Rx) and Transmitter (Tx) tagged.

Measures of channel performance and availability were retrieved for all the High Frequency (HF) transmited frequencies, from 2 to 30 MHz in steps of 500 kHz, at hourly samplings during the different Antarctic campaigns. Several studies have been conducted over the sounding data during the project as: (a) frequency/hour analysis of the oblique sounding results [8,9], (b) comparison with vertical sounding parameters [10] and (c) wideband measurements for communication purposes [7].

As stated in [11], there is a clear relation between the best successful transmitting frequencies and the sunspot numbers (SSN) which is a proxy of the solar activity reflecting the different solar variations and cycles. Other projects have been conducted to study the relations between the ionospheric channel and the Sun phenomena, as the presented by Angling et al. in 1999 [12]. The DAMSON sounder was used to determine the optimal transmission frequency set in adaptive HF systems. However, only links from 200 to 2000 km were tested, and longer links use larger sets of frequencies due to the different latitudes that need to be adapted [13].

This paper presents a study of the variation of the Signal-to-Noise Ratio (SNR) and availability of the 12,760 km ionospheric radio link for the last four-year campaigns measured over the data received in the inverted-V antenna, and it compares such variations to the solar activity proxy SSN. It also details the study of the narrowband-sounding performance using a monopole in transmission and the inverted-V antenna in the receiver; for information about the results of the narrowband sounding over the data received with the rugged monopole, see [10]. The interannual variation of the propagation parameters is evaluated taking into account different systematic measures from worldwide observatories in order to obtain relations between the solar activity phenomena and the channel availability of the ionospheric radio link.

This paper is organized as follows. Section 2 details the system description. Section 3 presents the narrowband sounding and Section 4 details the results. Afterwards, Section 5 discusses the results and, finally, Section 5 states the conclusions.

2. System Description

The system is a low power high frequency (HF) transceiver that monitors the ionospheric channel between the Antarctica and Spain. The sounder is fully configurable and can analyze different parameters from the ionospheric link at any frequency in the HF band. The system was designed to satisfy a project born in 2003 with a double objective: to transmit the data from remote sensors located at the Spanish Antarctic Station Juan Carlos I directly to Spain but implementing a long-haul oblique ionospheric sounder also. For more details on the system we refer the reader to [14,15].

The system is aimed to provide a reliable real-time connection for the remote sensors of the external environment located in the Antarctica. The system can be used to track and identify the human impact in this region as well as the ecosystem health, being an interesting contribution to the scientific community.

After some improvements of the system in the transmission block, a 7.5 m rugged monopole with radials was used after several software simulations [16]. Finally, 32 radials of 15 m length and 2.5 mm^2 section were used to improve 2 dB the gain in middle frequencies (15 MHz) (see Figure 2a). However, some additional isolation was required to avoid the electric arc caused by the increment of voltage drop between the antenna terminals. An antenna tuner is used by the transmitter to work in all frequencies without damaging the power amplifier. Still, on occasion, some components were burned when the antenna tuner retried to tune at full power. Hence, a Voltage Standing-Wave Ratio (VSWR) meter was designed to protect the power amplifier in case of malfunctioning in the tuning procedure. In reception, an inverted-V antenna is used with the subsequent filtering and amplification stages (see Figure 2b). No tuners are needed for this antenna. These later upgrades and a complete description of the system can be found in better detail in [10,15].

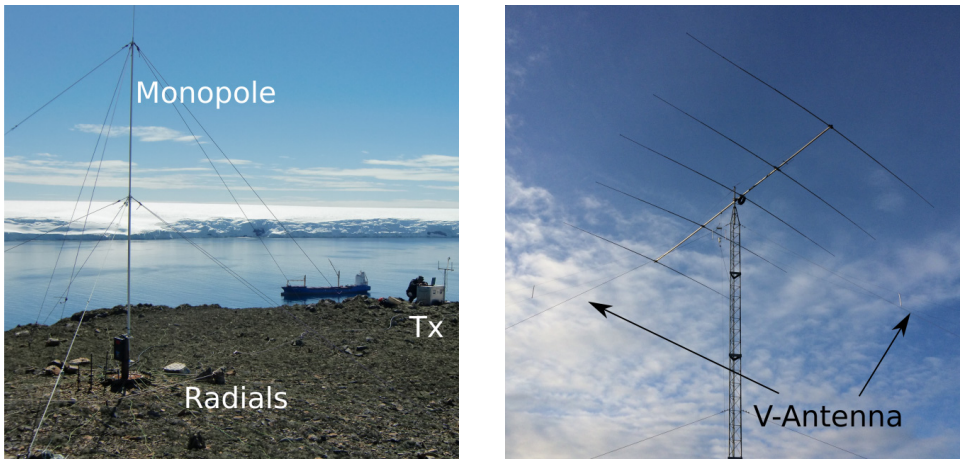

(**a**) (**b**)

Figure 2. (**a**) The transmitting antenna in the Antarctica, a 7.5 m rugged monopole with 32 radials; (**b**) The receiving antenna in Cambrils, the inverted-V antenna (see the two higher wires hanging from the big mast).

3. Narrowband Sounding

The aim of the narrowband sounding is to retrieve the SNR and the channel availability for the different time of the day and different frequency configurations to know the propagation characteristics of the ionospheric channel.

Narrowband soundings of the channel have been carried out hourly thanks to the flexibility of the hardware, whose Field-Programmable Gate Array (FPGA) allows the continuous frequency adaptation to the several frequencies using a plain-text configuration file [9]. The accuracy of the sounding frequencies and the time synchronization needed for narrowband soundings have been achieved thanks to the Oven-Controlled Crystal Oscillator (OCXO) and the Pulse per Second (PPS) signal of the GPS, respectively.

In order to find the Frequency of Largest Availability (FLA) of the channel, the frequencies from all the HF band have been tested in our modem. For this reason, frequencies ranging from 2 MHz to 30 MHz at 500 kHz steps have been analyzed for each of the 24 different hours of the day, resulting into a total of 1368 (57 freq. x 24 h) daily different combinations of measurements to analyze during all the antarctic survey for each year. The FLA represents the best transmitting frequency, the one showing the greater availability, for a given hour of a particular campaign.

The sounding is carried out continuously following a determined frame structure (as shown in Figure 3), where a tone of 10 s is sent hourly for all the frequencies every hour and everyday in the campaign.

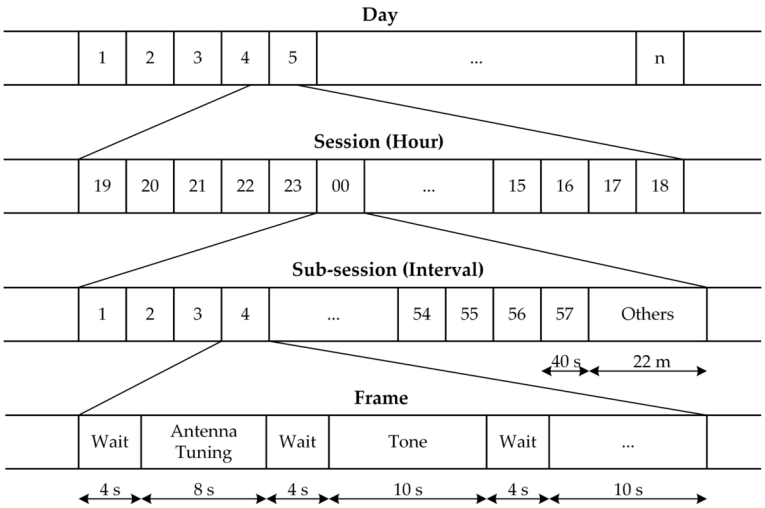

Figure 3. Diagram of sounding divided in hours, intervals and frames. In each hour, the 57 frequencies (from 2 MHz to 30 MHz in steps of 500 kHz) are tested in frames of 40 s.

SNR Measurement of the Narrowband Sounding

The SNR measurement is conducted as follows, and needs Figure 4 to be detailed. First, a filter is applied in frequency domain, after using the Fast Fourier Transform (FFT), to obtain a usable power profile. Afterwards, the windowing implemented removes the non-desired signals and avoids the transients from impulsive interferences. Also, a Kaiser windowing is applied because is presented a smoother response in several tests [9].

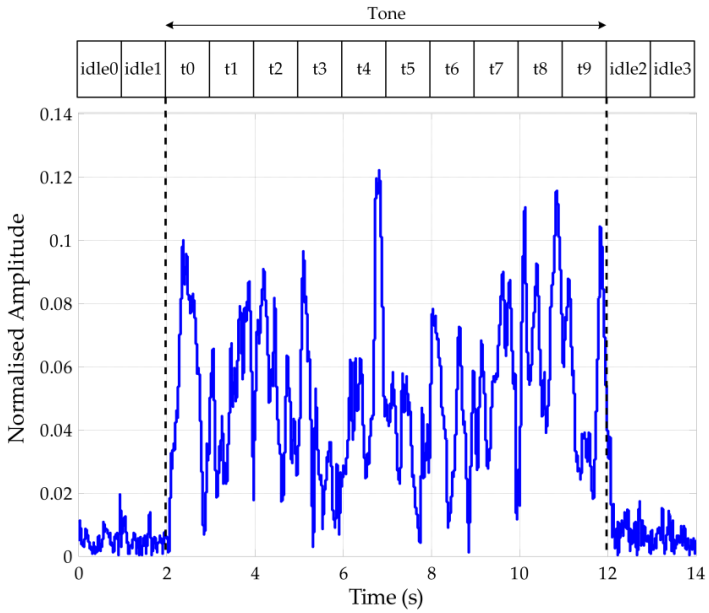

Figure 4. Schematic of the time-framing technique applied in the narrowband sounding. The idle spaces are used to measured the noise reference whereas the signal is measured in the tone slots.

Afterwards, it is computed dividing the measured tone power by the measured noise power, when no tone is sent. The channel availability is the probability for the link to reach a minimum SNR value, achieving a certain Quality of Service (QoS) [17]. A minimum value of 6 dB is defined in [8] in order to retrieve the channel availability in a bandwidth of 10 Hz. Thanks to several techniques developed in [9], the reliability of the detection system was improved and it gained invulnerability against high noise and interference.

To minimize the distortion of the SNR measurement, the following time-framing technique is applied (see Figure 4). It consists in dividing the tone frame into 10 intervals of one-second duration to observe the evolution of the SNR along the whole measurement (upper plot of Figure 4). It also includes two intervals of one second duration each to measure the noise before and after the measurement of the signal strength. The lower plot of Figure 4 shows an example of the diagram of the narrowband sounding for a real measurement. For more details about the narrowband sounding computation, see [7].

4. Results

In this section, the results for the comparison of the availability of the four last campaigns is shown, as well as a first approach to the analysis of variation of the propagation in function of the solar activity based on SSN.

4.1. Interannual Channel Availability

Table 1 shows the starting and ending dates with narrowband sounding measurements for the last four antarctic surveys. The fact that all the campaigns have so different number of days with available measurements depends on the meteorologically-driven expeditions by the Spanish National Research Council who manages the Spanish Antarctic Base Juan Carlos I and where the system is installed.

Table 1. Start and end days of measurements for the surveys carried out during the austral summer from 2011 to 2014.

Survey Name	Start Date	End Date
S. 2010-11	22 January 2011	01 March 2011
S. 2011-12	13 February 2012	25 February 2012
S. 2012-13	05 January 2013	24 February 2013
S. 2013-14	24 January 2014	18 February 2014

In order to analyze the year-by-year variation of our ionospheric radio link, we have evaluated the channel availability and particularly the FLA. The results for the individual surveys from 2011 to 2014 are depicted in Figure 5, where the channel availability is plotted in terms of percentage. This percentage, representing the availability, is computed using the number of observations that the SNR has a value over a threshold (6 dB), over the total amount of days of the campaign in a certain frequency at a certain hour. The daily variation of the FLA is plotted also as a black line, indicating the frequencies having the best availability for a given hour of each survey. As it can be observed from the results, the daily variation of the channel availability and of the FLA behaves different from one survey to each other.

We can distinguish four time intervals in relation to the daily variations of the channel availability: day, night, sunrise and sunset. During the day-time interval, from 08 UTC to 17 UTC approximately, the frequencies ranging from 18 to 30 MHz present the larger availability. The night-time interval, defined from 23 UTC to 06 UTC, shows that frequencies ranging from 6 to 13 MHz present the larger availability. Then, rapid changes are observed for time interval near sunrise, from 07 UTC to 09 UTC approximately, when frequencies with larger availability increase quasi-linearly with the time from frequencies between 6 and 13 MHz to frequencies ranging from 20 to 30 MHz. However, for time interval near-sunset, from 18 UTC to 22 UTC approximately, the frequencies with larger availability tends to decrease with time from 20 and 30 MHz to 10 and 20 MHz. Therefore, the higher frequency range have larger availability for day-time while lower frequency ranges behaves better for night-time in terms of channel availability. These results confirms the results pointed out in [10] and it extend to further surveys.

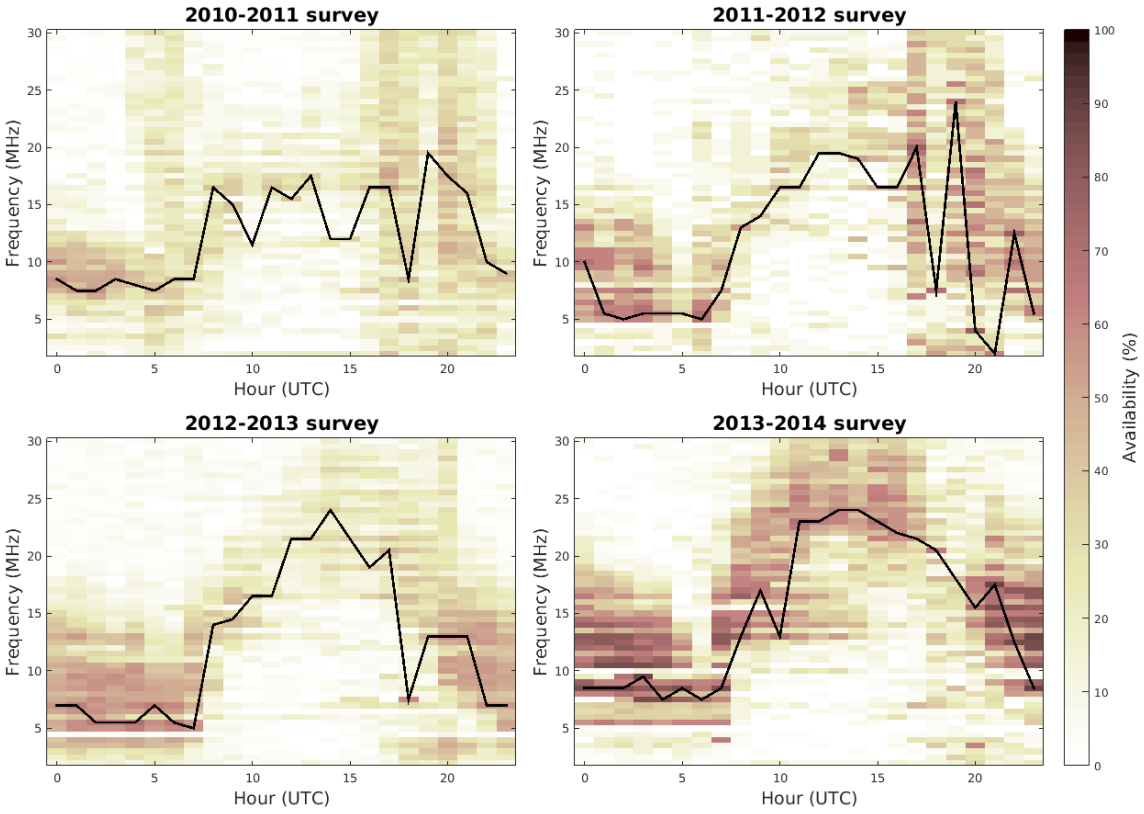

Figure 5. Cross-plots of the channel availability function of the time and frequency for the four antarctic surveys under study, result of the narrowband availability sounding over the receptions of the inverted-V antenna in Cambrils.

In terms of variation of the FLA, it shows lower values for 2010-11 campaign, and it increases its maximums during the day (from 08 UTC to 17 UTC approximately) as we reach campaigns 2011-12, 2012-13 and finally, 2013-14, which presents the higher FLA values. This is related to the propagation of the channel, which is also represented in Figure 5 with the availability. The lower availability also corresponds to the first campaign, and the higher availability to the last one. In order to analyze the possible influence of the solar activity on the channel availability variations, we depict in Figure 6 the time variations of the monthly-averaged SSN for the last five years (for more details visit [18]). Note that the months belonging to the last four surveys are marked in colors and tagged according the campaign they belong to. The average values of the solar activity proxy SSN corresponding to a given survey range from 20 to 80 units. That is why the channel availability for this particular radio link can be analyzed for low to mid solar activity conditions, increasing the possibility to analyze the channel performance for wider range of solar activity conditions. Figure 5 results show better results in terms of propagation as the monthly averaged sunspot number is higher, from a minimum of around 20 to a maximum of over 80.

As shown in Figure 6, the 2010-11 survey presents the lowest solar activity of the time interval under analysis (SSN ≈ 25) and it coincides with the worst channel availability rates (by 60% for the better FLA). Surveys 2011-12 and 2012-13 present similar solar activity and a bit larger than for survey 2010-11 (SSN ≈ 50). The channel availability for such surveys behave quite similar, being larger than that for survey 2010-11 (by 75% for the better FLA). The last analyzed survey, 2013-14, presents the best availability rates (by 85% for the better FLA), coinciding also with the highest solar activity interval analyzed (SSN ≈ 90).

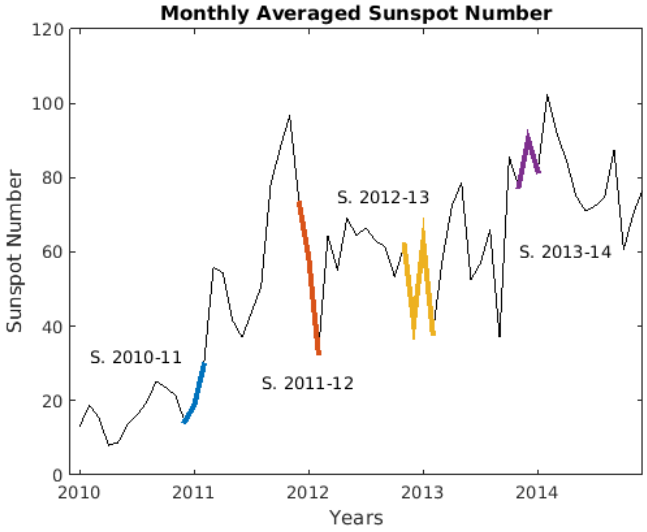

Figure 6. The monthly-averaged measure of the Sunspot Number provided by the Kandilli Observatory in the NOAA website [18].

In addition the FLA changes his daily variation as the solar activity changes from one survey to an other. Table 2 presents the detailed numbers of the FLA for a given hour and survey analyzed in this work, as well as the maximum availability for the given frequency. The values are extracted from Figure 5, and show clear differences between the availabilities of the different campaigns.

Table 2. FLA summary of the last four antarctic surveys. In bold, the FLA in MHz, and below, the percentage indicates the average availability for the FLA in the determined hours. Note that the time is presented in UTC. In color salmon, the daytime hours.

	UTC	**00**	**01**	**02**	**03**	**04**	**05**	**06**	**07**	**08**	**09**	**10**	**11**
2010-11	**MHz**	**8.5**	**7.5**	**7.5**	**8.5**	**8**	**7.5**	**8.5**	**8.5**	**16.5**	**15**	**11.5**	**16.5**
	Avail.	56%	56%	59%	51%	44%	46%	44%	36%	41%	41%	23%	41%
2011-12	**MHz**	**10**	**5.5**	**5**	**5,5**	**5.5**	**5.5**	**5**	**7,5**	**13**	**14**	**16.5**	**16.5**
	Avail.	69%	69%	62%	69%	62%	38%	69%	54%	54%	38%	46%	46%
2012-13	**MHz**	**7**	**7**	**5.5**	**5.5**	**5.5**	**7**	**5.5**	**5**	**14**	**14.5**	**16.5**	**16.5**
	Avail.	57%	63%	67%	65%	71%	63%	67%	57%	42%	45%	49%	29%
2013-14	**MHz**	**8.5**	**8.5**	**8.5**	**9,5**	**7.5**	**8.5**	**7.5**	**8.5**	**13**	**17**	**13**	**23**
	Avail.	85%	85%	85%	88%	85%	85%	73%	85%	77%	65%	69%	69%
	UTC	**12**	**13**	**14**	**15**	**16**	**17**	**18**	**19**	**20**	**21**	**22**	**23**
2010-11	**MHz**	**15.5**	**17.5**	**12**	**12**	**16.5**	**16.5**	**8.5**	**19.5**	**17.5**	**16**	10	**9**
	Avail.	41%	36%	28%	36%	46%	56%	46%	36%	51%	46%	46%	46%
2011-12	**MHz**	**19.5**	**19.5**	**19**	**16.5**	**16.5**	**20**	**7.5**	**24**	**4**	**2**	**12.5**	**5.5**
	Avail.	31%	31%	54%	46%	54%	77%	69%	69%	77%	62%	77%	62%
2012-13	**MHz**	**21.5**	**21.5**	**24**	**21.5**	19	**20.5**	**7,5**	**13**	**13**	**13**	**7**	**7**
	Avail.	33%	37%	35%	37%	37%	47%	61%	47%	61%	57%	57%	55%
2013-14	**MHz**	**23**	**24**	**24**	**23**	**22**	**21.5**	**20.5**	**18**	**15.5**	**17.5**	**12.5**	**8.5**
	Avail.	65%	65%	62%	69%	62%	58%	65%	46%	69%	88%	85%	88%

Shaded colons are distinguished in Table 2 to highlight the different daytime and nighttime intervals. Daytime, in UTC, occurs from 08 to 18 UTC approximately, where the FLA ranges between 15 and 23 MHz, depending on the survey. Nighttime is considered from 20 to 06 UTC, where the FLA varies between 6 and 9 MHz. In change regions between daytime and nighttime, during the sunrise and the sunset, an availability decrease can be observed.

It is clearly observed from Figure 5 and Table 2 that the average availability of the channel differs from one survey to the other noticeably. The average channel availability for the surveys S. 2010-11, S. 2011-12, S. 2012-13, and S. 2013-14, are 44%, 58%, 52%, and 74% respectively. Performing the last survey substantially better than the other and being the 2010-11 the worst one, in terms of channel

availability. Therefore, the increase of the solar activity results in a increase of the channel availability for this particular radio link. We may speculate that the higher solar activity, producing more ionization of the ionosphere results in better radio transmission from the Spanish Antarctic Base to Spain.

4.2. Interday SNR vs. SSN Variation

In this subsection we present the first results of the study of the relationship between the SNR evaluated in the channel and the variation of the solar activity proxy SSN. In order to do this, we estimate the cross-covariance [19] between the time series of the SNR of the channel for a given radio frequency and the time series of the solar activity SSN for all the days of the campaign. Cross-covariance analysis is used to evaluate the possible influence in the variations of one time series to another [20,21] in a very compact form.

In Figure 7 we can observe the result of the cross-covariance between the SNR and the SSN (shown in Figure 9) for 7 MHz in the campaign 2012-13, with the results plot in columns representing the hours of the day in UTC. There is a clear inverse dependency between the two variables, reaching maximums of -25 slightly delayed with respect to the perfect synchronization of the data. The mean delay of the minimum is 6.36 days respect the zero delay; the minimum delay is 2 days, and the maximum delay of 10 days. The channel variation depending on the SSN has a mean delay of around 6 days.

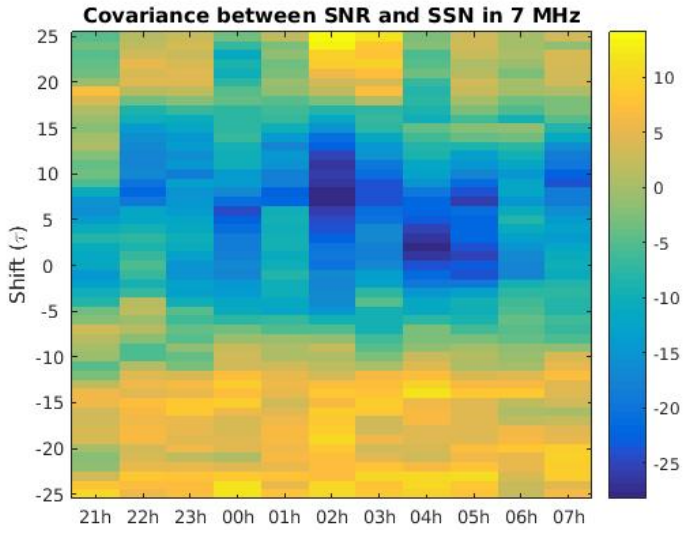

Figure 7. Cross-covariance between the SNR and the SSN in survey 2012-13, at 7 MHz.

In Figure 8, the results of the cross-covariance between the SNR and the SSN during the day are shown. They also perform a clear inverse dependency between the two variables. In this case, the minimum delay is of 6 days, and the maximum one is of 12 days, which makes a mean delay of 7,57 days. So, in this case, the effects over the channel propagation are also delayed with respect of the sun performance.

The propagation improves with higher SSN values due to ionization, but for large values of SSN it can occur the opposite effect. In Figure 9 the SSN of the analyzed days is shown, with large values the first days (around 8) and smaller values afterwards.

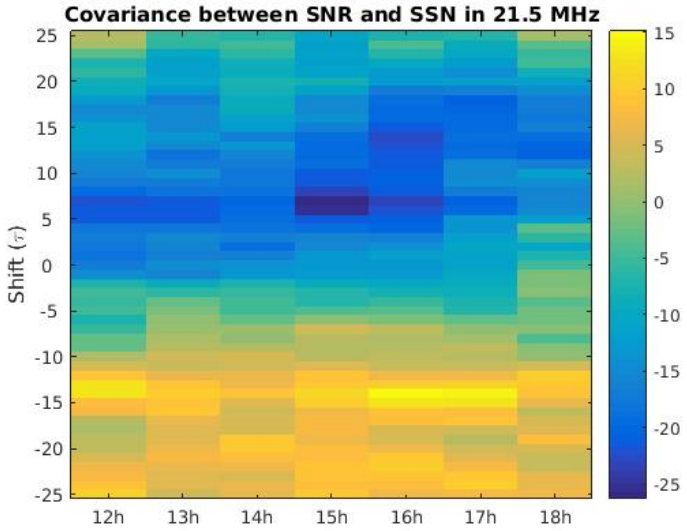

Figure 8. Cross-covariance between the SNR and the SSN in survey 2012-13, at 21.5 MHz.

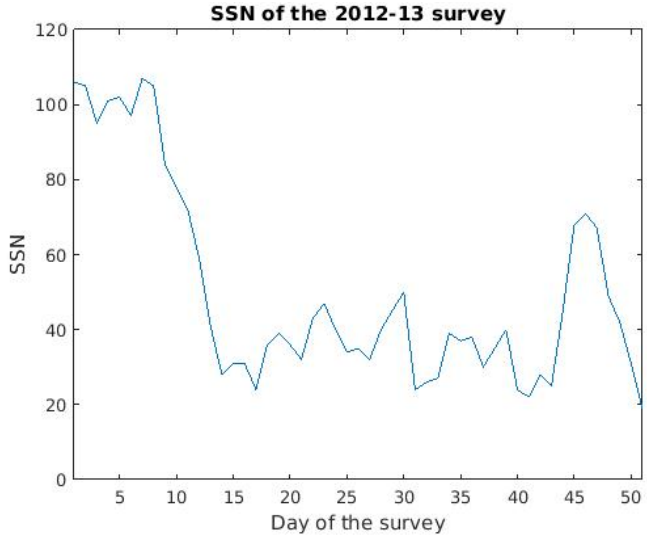

Figure 9. SSN index during the days of the 2013-14 survey.

5. Discussion

The analysis depicted in Section 3.1 shows a dependence of the global availability of the channel in function of the monthly averaged SSN value. This dependence is clear if we look at Figure 10, where the FLA for the last four campaigns is compared. The best transmission frequency for night hours is similar in all campaigns, but the frequencies for best propagation during the day have a strong dependence on the average SSN, showing a wider range of values. This leads us to the conclusion that the FLA for the use of the system as a modem might change depending on the average SSN of each campaign. In the past, the narrowband availability for this link had already been studied [3,4], but no comparison with the sun performance was made in those works.

In Figure 10, the FLA for the four campaigns is plotted to compare the differences between daytime and nighttime performance. Figures 11 and 12 show the detail of the performance of the FLA during daytime and during nighttime. Figure 11 plots the measured availability for each frequency of the FLA from 01 to 06 UTC. The results show that the higher FLA corresponds to 2013-14 campaign, and the lower ones to 2011-12. The four measured FLA show stable results for the four campaigns, with no severe variations during this nighttime.

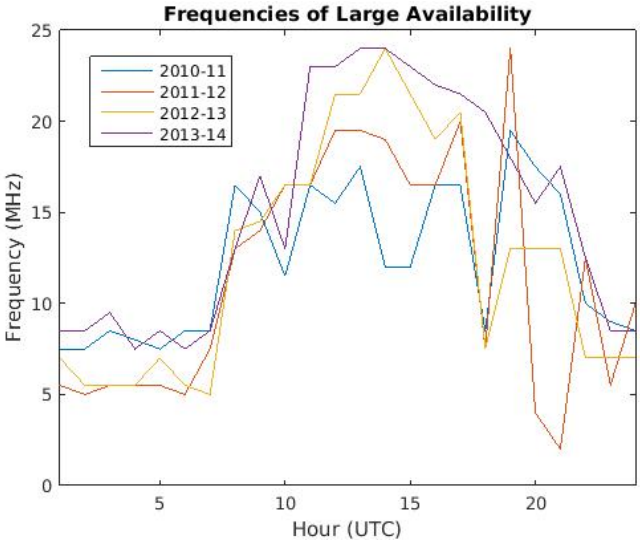

Figure 10. FLA of each hour for the last four surveys.

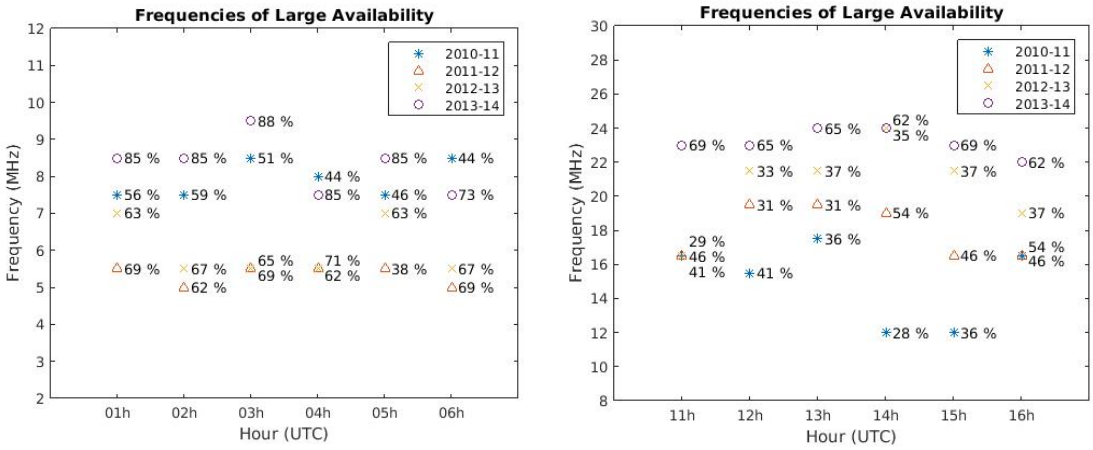

Figure 11. Detail of the FLA for the last four surveys: (**a**) from 01 h to 06 h UTC (**b**) from 11 h to 16 h UTC.

On the other hand, Figure 12 plots the same results for daytime (11 to 16 UTC), and some conclusions can be obtained from it. The higher FLA values correspond to 2013-14 campaign, with the higher SSN. They show the best availability results, around 60%, which is a high value for the hostile channel we are using. The mean availability decreases as the FLA, and also as the SSN value. In the daytime frequencies and availabilities it is clearer that the dependency of the maximum value of the FLA and the availability of the channel during an entire campaign with the performance of the sunspot number in the same period.

Comparing the performance of the four campaigns on daytime and nighttime, campaign 2010-11 performs high availability results for nighttime values (around 60%); we conclude that the reason is that low SSN improve the propagation at low frequencies, reaching better availabilities than other campaigns with higher SSN. The results of availability during daytime are lower (around 30%). Campaign 2011-12 performs in a similar way, with small availability values during the day and better values for the nighttime.

6. Conclusions

The narrowband propagation, represented in this work using the SNR of the 12,760 km transequatorial ionospheric channel, has a strong dependence on the solar variations due to its

influence in the ionospheric performance. This paper has shown two examples of this dependence. The first one is the comparison of the availability of the long-haul channel during a solar campaign (usually around 1 month long) with the monthly-averaged sunspot number. The conclusion for that study is that the higher the SSN, the better the performance of the channel. The second one studies the interday dependence, and uses the covariance between the SNR and the SSN. The results for this first attempt of covariance study show a strong inverse dependency of the SNR and the SSN values, both of them delayed around 6 days from the moment of the solar change to the channel propagation change. These first results encourage us to perform the same tests with other campaigns in order to reach an entire solar cycle description (around 11 years), as well as to increase the number of solar parameters to take into account in the study.

Acknowledgments: This work has been funded by the Spanish Government under the projects CGL2006-12437-C02, CTM2008-03536-E, CTM2009-13843-C02, and CTM2010-21312-C03. The authors would like to thank J.L. Pijoan and J.R. Regué, the Principal Investigators of these projects. The authors thank the Secretaria d'Universitats i Recerca del Departament d'Economia i Coneixement (Generalitat de Catalunya), under grant ref. 2014-SGR-0590, for funding partially the study that led to this paper.

Author Contributions: Ferran Orga conducted the interannual study of the availability, and also the interday covariance study of the SSN and the SNR of the link. He has also written most of the sections of the paper. David Altadill has leaded the analysis of the dependence of the availability and the SNR of the SSN, and has reviewed the paper. Marcos Hervás conducted the narrowband sounding analysis, and has reviewed the paper. Finally, Rosa Ma Alsina-Pagès has written part of the paper, and led the idea of the two comparative studies.

Conflicts of Interest: The authors declare no conflict of interest.

Abbreviations

The following abbreviations are used in this manuscript:

FFT	Fast Fourier Transform
FLA	Frequency of Largest Availability
FPGA	Field-Programmable Gate Array
GPS	Global Positioning System
HF	High Frequency
NLOS	Non-Line-Of-Sight
OCXO	Oven Controlled Crystal Oscillator
PPS	Pulse per Second
QoS	Quality of Service
SNR	Signal-to-Noise Ratio
SSN	Sunspot Number
TID	Traveling Ionospheric Disturbances
UTC	Coordinated Universal Time
VSWR	Voltage Standing-Wave Ratio

References

1. Rishbeth, H.; Garriott, O.K. *Introduction to Ionospheric Physics*; Academic Press: New York and London, 1969.
2. Angling, M.J.; Shaw, J.; Shukla, A.K.; Cannon, P.S. Development of an HF selection tool based on the Electron Density Assimilative Model near-real-time ionosphere. *Radio Sci.* **2009**, *44*, RS0A13, doi:10.1029/2008RS004022.
3. Forbes, J.M.; Palo, S.E.; Zhang, X. Variability of the ionosphere. *J. Atmos. Sol. Terr. Phys.* **2000**, *62*, 685–693, doi:10.1016/S1364-6826(00)00029-8.
4. Rishbeth, H.; Mendillo, M. Patterns of F2-layer variability. *J. Atmos. Sol. Terr. Phys.* **2001**, *63*, 1661–1680, doi:10.1016/S1364-6826(01)00036-0.
5. Altadill, D.; Apostolov, E.M. Time and scale size of planetary wave signatures in the ionospheric F region: Role of the geomagnetic activity and mesosphere/lower thermosphere winds. *J. Geophys. Res.* **2003**, *108*, 1403, doi:10.1029/2003JA010015.

6. Altadill, D.; Apostolov, E.M.; Boska, J.; Lastovicka, J.; Sauli, P. Planetary and gravity wave signatures in the F-region ionosphere with impact on radio propagation predictions and variability. *Ann. Geophys.* **2004**, *47*, 1109–1119, wos:000224826100012.
7. Hervás, M.; Alsina-Pagès, R.M.; Orga, F.; Altadill, D.; Pijoan, J.L.; Badia, D. Narrowband and Wideband Channel Sounding of an Antarctica to Spain Ionospheric Radio Link. *Remote Sens.* **2015**, *7*, 11712–11730, doi:10.3390/rs70911712.
8. Vilella, C.; Miralles, D.; Pijoan, J.L. An Antarctica-to-Spain HF Ionospheric Radio Link: Sounding Results. *Radio Sci.* **2008**, *43*, 1–17, doi:10.1029/2007RS003812.
9. Ads, A.G.; Bergadà, P.; Vilella, C.; Regué, J.R.; Pijoan, J.L.; Bardají, R.; Mauricio, J. A Comprehensive Sounding of the Ionospheric HF Radio Link from Antarctica to Spain. *Radio Sci*. **2012**, *48*, 1–12, doi:10.1029/2012RS005074.
10. Ads, A.G.; Bergadà, P.; Regué, J.R.; Alsina-Pagès, R.M.; Pijoan, J.L.; Altadill, D.; Badia, D. Vertical and Oblique Ionospheric Soundings over the Long Haul HF Link between Antarctica and Spain. *Radio Sci*. **2015**, doi:10.1002/2015RS005773.
11. Ostrow, S.; Po-Kempner, M. The differences in the relationship between ionospheric critical frequencies and sunspot number for different sunspot cycles. *Tran. IRE Prof. Group Antennas Propag.* **1952**, *57*, 473–480, doi:10.1029/JZ057i004p00473.
12. Angling, M.J.; Davies, N.C. An assessment of a new ionospheric channel model driven by measurements of multipath and Doppler spread. In Proceedings of the 1999 IEEE Colloquium on Frequency Selection and Management Techniques for HF Communications, London, UK, 29–30 March 1999.
13. Cannon, P.S.; Angling, M.J.; Davies, N.C.; Wilink, T.; Jodalen, V.; Jacobson, B.; Lundborg, B; Broms, M. Damson HF channel characterization—A review. *MILCOM* **2000**, *1*, 59–64, doi:10.1109/MILCOM.2000.904913.
14. Bergadà, P.; Deumal, M.; Vilella, C.; Regué, J.R.; Altadill, D.; Marsal, S. Remote sensing and skywave digital communication from Antarctica. *Sensors* **2009**, *9*, 10136–10157, doi:10.3390/s91210136.
15. Pijoan, J.L.; Altadill, D.; Torta, J.M.; Alsina-Pagès, R.M.; Marsal, S.; Badia, D. Remote Geophysical Observatory in Antarctica with HF Data Transmission: A Review. *Remote Sens.* **2014**, *6*, 7233–7259, doi:10.3390/RS6087233.
16. Alsina-Pagès, R.M.; Hervás, M.; Orga, F.; Pijoan, J.L.; Badia, D.; Altadill, D. Physical layer definition for a long-haul HF Antarctica to Spain radio link. *Remote Sens.* **2016**, *8*, 380, doi:10.3390/rs8050380.
17. Goodman, J.; Ballard, J.; Sharp, E. A long-term investigation of the HF communication channel over middle- and high-latitudes paths. *Radio Sci.* **1997**, *32*, 1705–1715, doi:10.1029/97RS01194.
18. Space Weather, National Centers for Environmental Information of the NOAA. Available online: http://www.ngdc.noaa.gov/stp/spaceweather.html (accessed on 6 June 2016).
19. Jenkins, G.M.; Watts, D.G. *Spectral Analysis and Its Applications*; Holden-Day: San Francisco, CA, USA, 1969.
20. Altadill, D. On the 18-day quasi-periodic oscillation in the ionosphere. *Ann. Geophys.* **1996**, *14*, 716–724, doi:10.1007/s00585-996-0716-0.
21. Jakowski, N.; Stankov, S.M.; Wilken, V.; Borries, C.; Altadill, D.; Chum, J.; Buresova, D.; Boska, J.; Sauli, P.; Hruska, F.; *et al.* Ionospheric Behaviour over Europe during the Solar Eclipse of 3 October 2005. *J. Atmos. Terr. Phys*. **2008**, *70*, 836–853.